Electronic Supplementary Information

Bromoargentate/g-C_3N_4 heterojunction by in situ growth: 2-D bromoargentate framework with a transition metal complex linker and cocatalyst for enhanced photocatalytic activity via g-C_3N_4 hybrid

Yiming Tian, Taohong Ren, Hongjin Zhu, Dingxian Jia*

College of Chemistry, Chemical Engineering and Materials Science, Soochow University, Suzhou 215123, People's Republic of China.

1. General methods

Elemental analysis (EA) of C, H and N was performed using an EA1110-CHNS-O elemental analyzer. Fourier transform infrared (FT-IR) spectra were recorded using a Nicolet Magna IR 550 spectrometer in the range of 4000-400 cm^{-1} using dry KBr disks. Powder X-ray diffraction (PXRD) data were collected on a D/MAX-3C diffractometer using graphite monochromatic Cu-Kα radiation (λ = 1.5406 Å). UV/Vis spectrophotometer. Scanning electron microscopy (SEM), and energy dispersive spectroscopy (EDS) of X-ray were obtained using a Hitachi S-4700 cold field emission scanning electron microscope at a voltage of 15.0 kV. X-ray photoelectron spectroscopy (XPS) measurements were recorded on an ESCALAB 250XI spectrometer equipped with a monochromatic Al *Kα* X-ray source (1486.6 eV). Optical diffuse reflectance spectra of powder samples at room temperature were determined by a Shimadzu UV-3150 spectrometer scanning photometer. The absorption data are calculated by reflectivity, using the Kubelka-Munk function $F(R) = (1–R)^2/2R$, where R is the reflectance at a given energy.[1]

Reference

[1] W.W. Wendlandt, H.G. Hecht, Reflectance Spectroscopy, Interscience Publishers, New York, 1966.

2. Photoelectric properties

The photocurrent reponses were measureed on a CHI760E electrochemical workstation using the standard three electrode method, with the sample coated ITO glass as the working electrode, the Pt wire as the auxiliary electrode, and the saturated calomel electrode (SCE) as the reference electrode. 15 mg of the sample was dispersed in a mixed solution of ethanol (0.5 mL) and 2 drops of Nafion, followed by sonication for 0.5 h. The above slurry was uniformly coated on ITO glass with an effective area of 1 cm^2, and naturally dried at room temperature. The high-voltage xenon lamp is located 20 cm from ITO electrode surface, and a Na_2SO_4 (0.1 $mol \cdot L^{-1}$) aqueous solution is used as the support electrolyte. In the cyclic voltammetry test, the working electrode was a glassy carbon electrode (GC) with a diameter of 1 cm, and the supporting electrolyte solution was NaOH (0.05 $mol \cdot L^{-1}$) solution.

3. **Photocatalytic experiments.**

The photocatalytic activities of compounds **1** and **1**/g-C_3N_4 composite for the degradation of CV were studied under visible light irradiation with a 180 W xenon lamp. The photocatalysts (25 mg) were added to an aqueous solution of CV (1×10^{-5} $mol \cdot L^{-1}$) and stirred for 30 min in the dark to reach an adsorption/desorption equilibrium. The vertical distance between the dye solution interface and the xenon lamp source was kept at 10 cm. During the photodegradation, about 4 mL of suspension was removed from the reaction at certain time interval and separated by centrifugation for UV-vis absorption spectroscopy measurements. The UV-vis absorption spectra of the dye solutions were measured on a PE Lambda 35 UV/vis spectrophotometer. In addition, blank experiments for the photocatalytic degradation of CV were carried out under the same conditions.

Table S1 Crystallographic data and refinement parameters of compound **1**

Compound	**1**
Empirical formula	$C_{24}H_{18}N_4O_2Cu_2Ag_3Br_5$
Formula weight	1244.66
Dimensions (mm)	0.20 × 0.10 × 0.10
Crystal system	triclinic
Space group	$P\bar{1}$
a (Å)	10.4752(15)
b (Å)	10.9876(15)
c (Å)	14.3813(19)
α (°)	110.378(4)

β (°)	107.663(4)
γ (°)	92.224(5)
V (Å)^3	1459.0(4)
Z	2
T (K)	296(2)
Dc (g/cm^3)	2.833
F (000)	1160
μ (mm^{-1})	10.290
θ range (°)	2.64 to 25.35
Unique reflns	53670
Rint	0.1263
Measured reflections	4323
Parameters	361
$R1$, [$I \geq 2\sigma(I)$]	0.0482
$wR2$, (all data)	0.1311
$\Delta\rho_{max}/\Delta\rho_{min}$ (e Å^{-3})	1.573/-1.229
GOF on F^2	1.093

Table S2. Selected Bond Lengths (Å) and Angles (°) for **1**

Ag(1)–Br(1)	2.6864(11)	Ag(1)–Br(1)#2	2.7649(12)
Ag(1)–Br(3)	2.6866(12)	Ag(1)–Br(5)#1	2.7377(12)
Ag(2)–Br(1)#2	2.8261(12)	Ag(2)–Br(2)	2.5827(11)
Ag(2)–Br(3)	2.8415(13)	Ag(2)–Br(4)	2.6753(12)
Ag(3)–Br(3)	2.7517(12)	Ag(3)–Br(4)	2.5837(12)
Ag(3)–Br(5)	2.6753(12)	Ag(3)–Br(5)#1	2.7540(12)
Ag(3)–Ag(3)#1	3.0726(15)	Cu(1)–Br(1)	2.9264(13)
Cu(1)–O(1)	1.919(5)	Cu(1)–O(2)	1.963(5)
Cu(1)–N(1)	2.009(7)	Cu(1)–N(2)	2.005(6)
Cu(2)–O(1)	1.927(5)	Cu(2)–O(2)	1.966(5)
Cu(2)–O(2)#3	2.381(5)	Cu(2)–N(3)	2.024(6)
Cu(2)–N(4)	1.996(7)		
Br(1)–Ag(1)–Br(1)#2	98.08(4)	Br(1)–Ag(1)–Br(3)	134.96(5)
Br(1)–Ag(1)–Br(5)#1	98.16(4)	Br(3)–Ag(1)–Br(1)#2	99.54(4)
Br(3)–Ag(1)–Br(5)#1	98.67(4)	Br(5)#1–Ag(1)–Br(1)#2	133.97(5)
Br(1)#2–Ag(2)–Br(3)	94.51(3)	Br(2)–Ag(2)–Br(1)#2	105.11(4)
Br(2)–Ag(2)–Br(3)	114.95(4)	Br(2)–Ag(2)–Br(4)	118.23(4)
Br(4)–Ag(2)–Br(1)#2	116.38(4)	Br(4)–Ag(2)–Br(3)	105.46(4)
Br(3)–Ag(3)–Br(5)#1	96.71(3)	Br(3)–Ag(3)–Ag(3)#1	104.35(4)
Br(4)–Ag(3)–Br(3)	110.75(4)	Br(4)–Ag(3)–Br(5)	121.52(4)
Br(4)–Ag(3)–Br(5)#1	113.43(4)	Br(4)–Ag(3)–Ag(3)#1	144.25(5)
Br(5)–Ag(3)–Br(3)	99.45(4)	Br(5)–Ag(3)–Br(5)#1	111.08(3)

Br(5)–Ag(3)–Ag(3)#1	56.75(3)	Br(5)#1–Ag(3)–Ag(3)#1	54.33(3)
Ag(1)–Br(1)–Ag(1)#2	81.92(3)	Ag(1)–Br(1)–Ag(2)#2	153.56(4)
Ag(1)#2–Br(1)–Ag(2)#2	72.72(3)	Ag(1)–Br(1)–Cu(1)	107.03(4)
Ag(1)#2–Br(1)–Cu(1)	168.20(5)	Ag(2)#2–Br(1)–Cu(1)	99.14(4)
Ag(1)–Br(3)–Ag(2)	73.63(3)	Ag(1)–Br(3)–Ag(3)	73.81(3)
Ag(3)–Br(3)–Ag(2)	68.79(3)	Ag(3)–Br(4)–Ag(2)	73.85(3)
Ag(1)#1–Br(5)–Ag(3)#1	72.98(3)	Ag(3)–Br(5)–Ag(1)#1	120.79(4)
Ag(3)–Br(5)–Ag(3)#1	68.92(3)	O(1)–Cu(1)–N(1)	96.6(2)
O(1)–Cu(1)–N(2)	172.7(3)	O(1)–Cu(1)–O(2)	82.2(2)
O(1)–Cu(1)–Br(1)	101.74(18)	O(2)–Cu(1)–N(1)	161.3(2)
O(2)–Cu(1)–N(2)	96.3(2)	O(2)–Cu(1)–Br(1)	111.69(16)
N(2)–Cu(1)–N(1)	82.5(3)	N(2)–Cu(1)–Br(1)	85.48(19)
N(1)–Cu(1)–Br(1)	86.87(18)	O(1)–Cu(2)–O(2)	81.9(2)
O(1)–Cu(2)–O(2)#3	100.1(2)	O(1)–Cu(2)–N(3)	164.9(3)
O(1)–Cu(2)–N(4)	97.6(2)	O(2)–Cu(2)–O(2)#3	84.5(2)
O(2)–Cu(2)–N(3)	97.6(2)	O(2)–Cu(2)–N(4)	177.0(3)
N(3)–Cu(2)–O(2)#3	94.9(2)	N(4)–Cu(2)–O(2)#3	98.5(2)
N(4)–Cu(2)–N(3)	82.1(3)		

Symmetry transformations used to generate equivalent atoms: #1) –x+1, –y+1, –z+1; #2) –x+1, –y+2, –z+1; #3) –x+1, –y+2, –z+2.

Table S3 Selected H···A distances (Å) and D–H···A angles (°) for **1**

D–H···A	d(H···A)	d(D···A)	<(DHA)
C(1)–H(1)···Br(4)#1	3.008	3.695	131.96
C(9)–H(9)··· Br(2)#3	3.005	3.844	150.82
C(10)–H(10)··· Br(2)#2	3.009	3.847	150.71
C(13)–H(13)··· Br(2)#2	2.944	3.461	116.51
C(21)–H(21)··· Br(3)#1	2.964	3.699	136.95

Symmetry transformations used to generate equivalent atoms: #1) –x+1, –y+1, –z+1; #2) –x+1, –y+2, –z+1; #3) x, y+1, z+1.

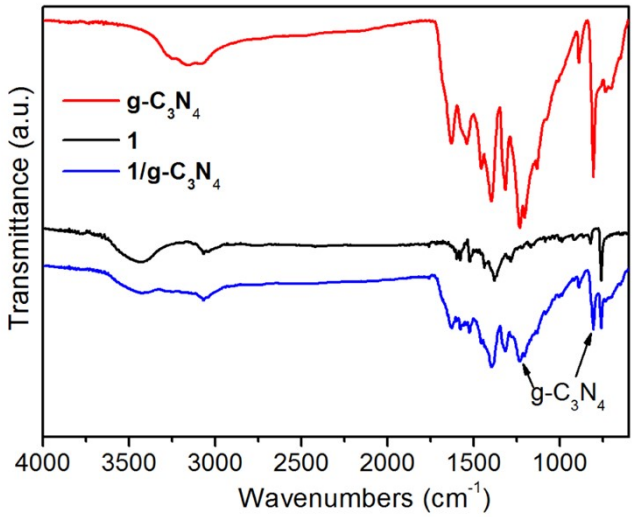

Fig. S1 FT-IR spectra of g-C_3N_4, **1** and **1**/g-C_3N_4 composite.

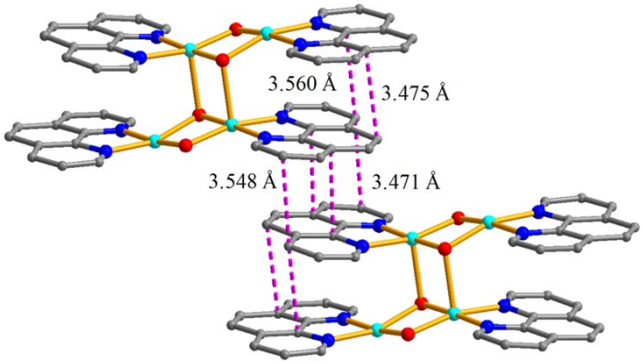

Fig. S2 A view of π···π interactions between the $[(\{Cu(phen)\}_2(\mu\text{-}OH)_2)(Ag_3Br_5)]_n$ layers in **1**.

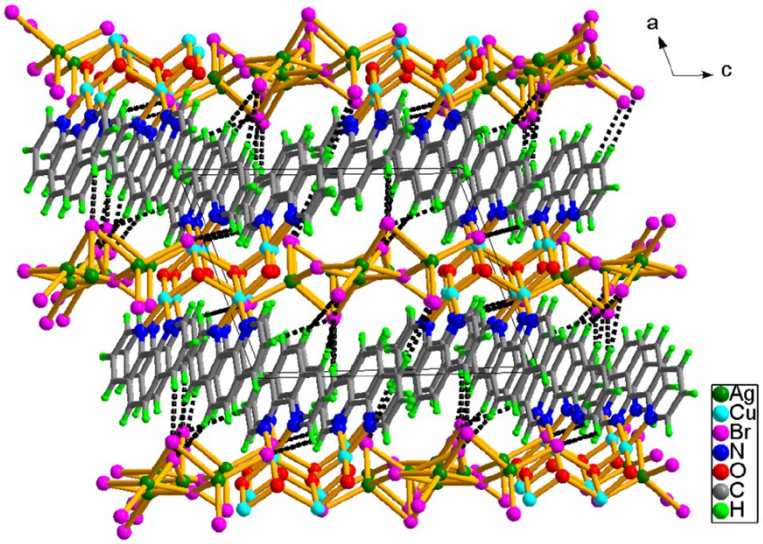

Fig. S3 Packing diagram of **1** viewed along the *b* axis, showing weak C–H···Br interactions between the

$[(\{Cu(phen)\}_2(\mu\text{-}OH)_2)(Ag_3Br_5)]_n$ layers in **1**.

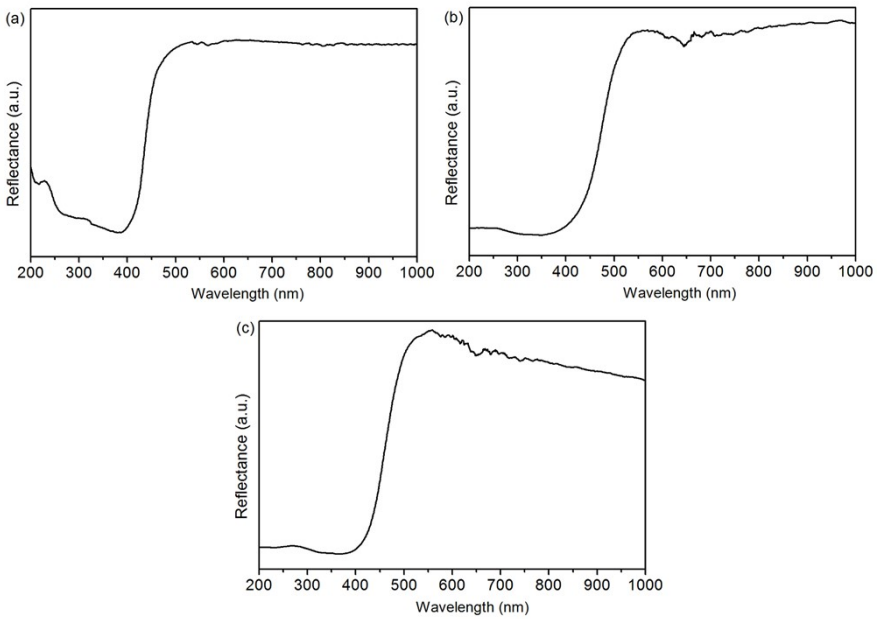

Fig. S4 Solid-state UV-Vis-NIR diffuse reflectance spectra of g-C_3N_4 (a), **1** (b) and **1**/g-C_3N_4 (c).

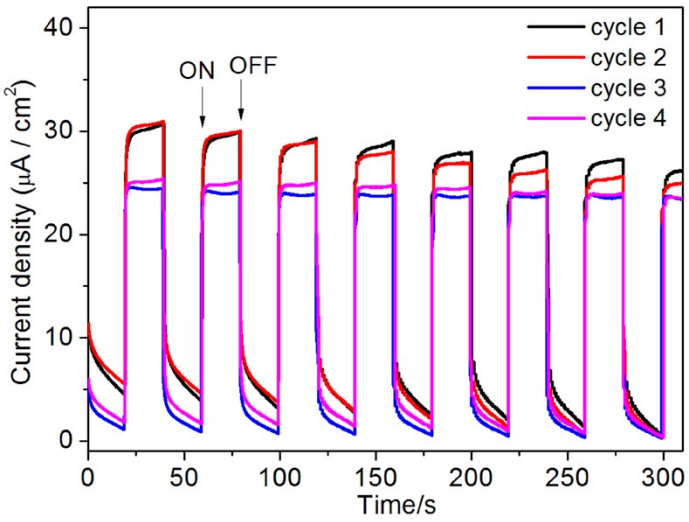

Fig. S5 Photocurrent responses of **1**/g-C_3N_4 heterojunction under illumination with light power of 150 W for four cycle measurements.

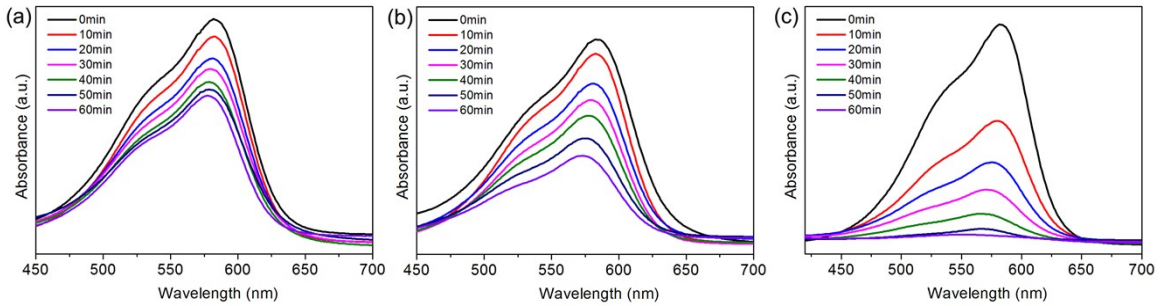

Fig. S6 Time dependent absorption spectra of CV solution with photodegradation catalyzed by g-C_3N_4 (a), **1** (b), and **1**/g-C_3N_4 heterojunction (c).

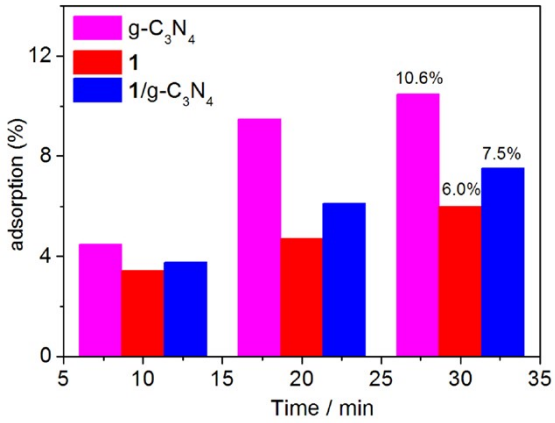

Fig. S7 Adsorption of CV in the presence of g-C_3N_4, **1** and **1**/g-C_3N_4 at different time intervals.

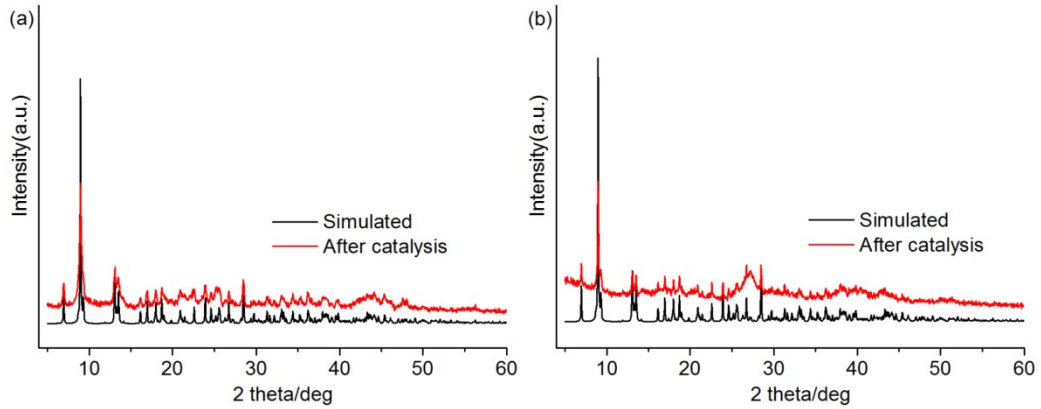

Fig. S8 Simulated PXRD patterns of compound **1**, and experimental PXRD patterns after photocatalysis of compound **1** (a) and **1**/g-C_3N_4 heterojunction (b).

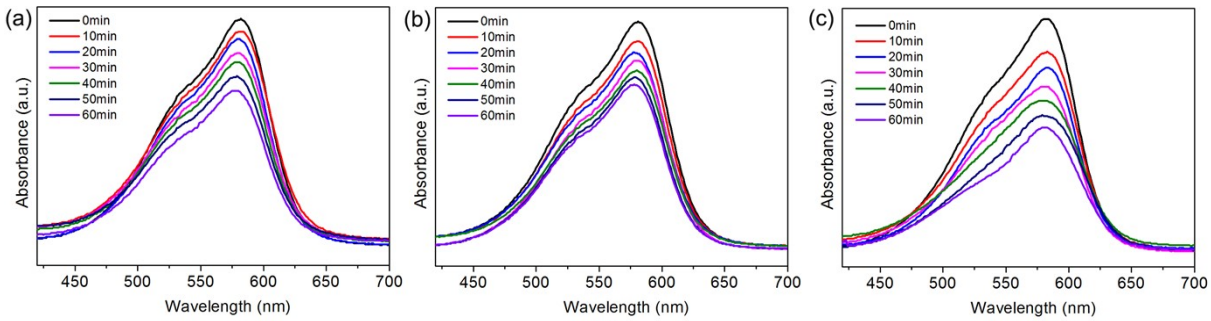

Fig. S9 Time dependent absorption spectra of MB solution with photodegradation catalyzed by **1**/g-C_3N_4 heterojunction in the presence of quenchers of BQ (a), AO (b), and TBA (c).

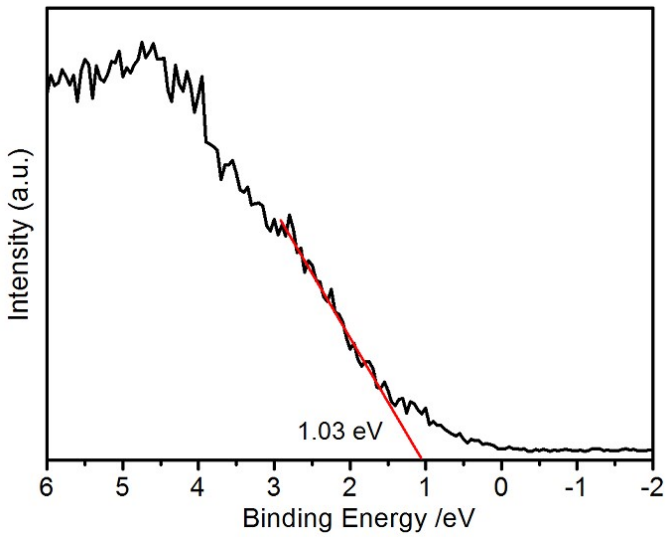

Fig. S10 Valence band XPS result of the compound **1**.